Simulazione dell'impatto di un bore mediante il moto a potenziale
A potential flow solver for bore impact

Enrico Bertolazzi e Filippo Trivellato

Department of Mechanical and Structures Engineering,

Department of Civil and Environmental Engineering,

University of Trento, Italy

Enrico.Bertolazzi@ing.unitn.it *Filippo.Trivellato@ing.unitn.it*

Abstract

The knowledge of the hydrodynamic loading due to the impact of a bore on a wall is crucial in the rational design of protection structures. The numerical modeling of an inviscid dam–break surge as it advances over a dry bed and strikes a wall is new in literature.

The aim of the present work is to present a finite volume element method, combined with a Crank-Nicolson scheme for time step advancing, that is capable of calculating the unsteady, incompressible, free surface flow field due to the collision of a bore on a vertical plane wall. The surge propagates along a dry bed and the 2–D impact is modeled by a fully nonlinear potential approach. A discrete formulation is implemented to trace accurately the pathline of the nodes on the free surface.

By conjecturing realistic initial conditions, the present numerical approach proved successful in obtaining a quantitative evaluation of physical quantities, such as the maximum force acting on the wall, so that meaningful predictions for wall pressures and wall force can be obtained not only from laboratory tests but also from numerical simulations.

The effect of air entrainment in the bore is briefly discussed.

1 Introduction

The impacting steady flow is herein referred to as *jet*, while the unsteady flow is termed as *bore*. The literature devoted to the many occurrences of the water impact phenomenon is large and exhaustive results have been collected, but none in the case of a bore *generated by a dam–break* and propagating along a *dry* bed, if exception is made for the laboratory physical experiments performed by (14) and (15). The papers that are more closely related to the present work are only those of (2), (11) and (7). The presence of water in the channel ahead of the surge does affect the shape of the wave tip as well as the generation of forces (2); the experimental results of (11) are relevant to assess the force experienced by a vertical wall due to the impact of a bore generated by a broken solitary wave and propagating over a liquid bath at rest; (7) solved the Euler's equations for the impact of a bore propagating over a static liquid bath.

The knowledge of the dynamic loading is crucial in the rational design of transversal structures; nowadays the assessment of dynamic loading is still founded mostly upon both past experience and field observations. The aim of this work is to verify whether an analytical approach, simpler than (7)'s and based on a potential flow solver, can describe the complex dynamics of the bore impact and to what extent can a potential model be accurate in obtaining wall forces. The 2–D impact of a plunging wave on a rigid vertical wall has been already simulated in the contest of potential flow by (16).

2 Experimental results

Physical experiments were conducted at the Hydraulic Laboratory of the University of Trento (Italy) that were originally intended to simulate debris–flow collisions on walls. The experimental apparatus comprised 6 meter long tilting flume and the flume slopes varied from 0° through 25°; the flume cross–section was $0.5\,m$ wide and $0.5\,m$ deep. In the upstream part of the flume, a mixture of granular material and water was released into the flume to generate a bore, which then advanced in a dry bed. The downstream part of the flume was made of a transverse wall that was instrumented with four gauges to measure impact pressures. The diameter of the *flush–to–the–wall* pressure membrane was $1\,cm$; a frequency response of $250\,Hz$ turned out to be convenient in recording the unsteady phenomenon. The measured pressures could reach $25\,kPa$. In spite of the great effort dedicated in performing accurate experiments, a poor repeatability was detected in the tests: in fact, the difference in pressure intensities among experiments sharing the same initial

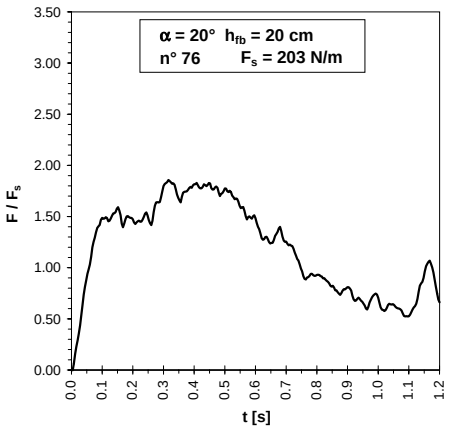

Figure 1: Example of wall force evolution.

conditions was as high as $5\% \div 15\%$. This observation is consistent with what already claimed by a number of authors, (3), (16) and (5). Poor repeatability was mostly due to the ever–changing evolution of the breaking front, the structure of which has strong 3-D patterns. Toe velocities u_o and toe depths h_f of the bore near the wall were measured by a video–recording apparatus (SVHS video–camera, 25 frames per second, shuttering time $1/1000\,s$). The measurements of *instantaneous* toe velocities were performed by tracing the location of the most advanced part of the ever–breaking front rushing downstream. The measured duration of the impact was found to be in accordance with known values of similar phenomena, e.g., plunging waves on vertical sea–walls, (11), (16).

As opposed to near–breaking sea waves impacts, in the experimental tests no trapping of an air pocket between the surge and the wall was observed. Important secondary circulations are generated at the instant of impact and massive air entrainment occurs in the liquid toe before and after the impact; due to the above phenomena, the temporal evolution of the wall pressure is pulsating. Typical features of the laboratory impacts are (fig. 1): (i) an initial sharp peak of force of short duration ($\sim 10^{-1}\,s$); (ii) a pulsating force of long duration ($\sim 1\,s$), normally decaying with time; (iii) a final peak of force of short duration ($\sim 10^{-1}\,s$), due to the collapsing of the run–up jet down onto the incoming surge at the bottom. This last peak has been found to be less severe than the first one, as opposed to the case of tsunami and sea bores, (2), (11).

As already claimed by (9), the thin crest of the run–up jet contributes nothing to the force at the wall; thus the time of the maximum run–up follows

the time the force attains its maximum.

The phenomenon of air entrainment is one of the major features occurring during the propagation of the dam–break bore; the phenomenon is particularly developed in the ever–breaking front wave rushing downstream, even for a surge propagating along a horizontal bottom. In the rear region, the flow pattern is definitely more organized and most of the turbulence generated in the toe region is dissipated. The rear flow pattern evolves towards superficial self–aeration, i.e. air is entrained only at the free surface. Effects of air entrapment are flow bulking and reduction of the bore density which becomes smaller than that of the pure water.

Prediction formulae of literature are only available for uniform or gradually varied flows and therefore cannot be extended meaningfully to the present instance of unsteady motion either in the front or in the rear region. The pressures measured in laboratory physical experiments should correspond to smaller values in the prototype where air entrainment is greater and the density of the air–water mixture is less than that of the pure water; (10) found a large reduction in pressure even for small air content. However, in spite of the pressure reduction, the total force acting on the wall is likely unmodified since air entrainment increases bulking but at the same time it decreases the mixture density, so that the total liquid mass involved in the collision – and the total momentum likewise – is expected to be basically unchanged.

The following simplified reasoning can be of help in understanding the constancy of the momentum. In case of no air entrainment, the momentum flux of the bore as it advances along a horizontal bed is written as:

$$M = \rho Q u_o = \rho u_o^2 h_f$$

The same quantity in case of air entrainment should be intended instead as:

$$M_m = \rho_m u_o^2 h_{fm}$$

where the subscript m stands for mixture (of air–water) and where it is assumed in the first approximation that u_o is not changed by the presence of air. The ratio between the two momentum equations becomes:

$$\frac{M_m}{M} = \frac{1 - 1.1\,C}{1 - C}, \quad C = \frac{V_a}{V_a + V_w} \quad (0.2 \leq C \leq 0.85)$$

where C is the mean air concentration and V_a, V_w are the volumes of air and water respectively; use has been made of the relations given by (12) that holds true for evenly distributed air in the liquid and for chutes having

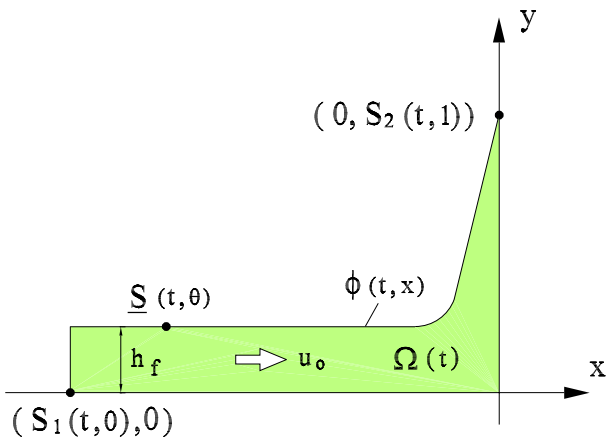

Figure 2: Sketch of the problem and notation.

rectangular cross sections. Both hypotheses are valid in the present contest. The bore thrust is not remarkably affected by air–entrainment as long as air concentration in the toe is as high as, just to fix the ideas, 0.3. Of course the above reasoning is correct only if applied to steady state conditions but it seems reasonable to extend it in the first approximation to unsteady motion as well.

3 Analytical formulation of the problem

A clear water bore hitting upon a rigid, vertical, plane wall is considered herein. The surge is generated by a dam break and propagates over a dry horizontal bed. It is to be reminded that there seem to be no rigorous results of general value in non–linear unsteady problems with both a free streamline (a streamline which separates fluid in motion from fluid at rest) and a contact line. Some simplifying hypotheses must therefore be formulated.

The first one concerns the compressibility of pure water that does not play a significant role in this kind of impact (9); also inertia forces are regarded by far dominant as compared to surface tension, viscosity and gravity forces. The dynamic interaction of a structure with a liquid jet should be solved in principle as a unified hydro–elastic system; however, the elastic response of the structure would pose additional complexities in the computations and therefore the wall has been regarded as a rigid body in the present simulation. After all, calculated pressures would be on the safety side; in fact, a pressure overestimation of only $3\% \div 6\%$, as compared to the more realistic case of

elastic wall, was claimed by (16). Hence, assuming further that the flow is irrotational and time–dependent in a simply connected domain, bounded by impervious walls and a free streamline, it is clear that the essential features involved in the collision process are described by a simplified approach based on the potential flow theory.

The computational liquid domain $\Omega(t)$ is assumed to be simply connected and time dependent (fig. 2). Its boundary, defined as $\partial\Omega(t) = \Gamma_s(t) \cup \Gamma_w(t)$, includes the free surface $\Gamma_s(t) = \{\mathbf{S}(t;\theta) \mid 0 \leq \theta \leq 1\}$ and the rigid, impermeable wall boundary $\Gamma_w(t) = \{(x,0) \mid S_1(t;0) \leq x \leq 0\} \cup \{(0,y) \mid 0 \leq y \leq S_2(t;1)\}$, where $\mathbf{S}(t;\theta)$ –the components of which are $S_1(t;\theta)$ and $S_2(t;\theta)$– is the parametric form of the *moving* free streamline, which can be not univocal; θ is a parameter running in the closed interval $[0,1]$. The velocity potential $\Phi = \Phi(t,\mathbf{x})$ satisfies Laplace's equation in the domain $\Omega(t)$ at any time t, supplemented by suitable boundary conditions:

$$\begin{cases} \nabla^2\Phi(t,\mathbf{x}) = 0, & \mathbf{x} \text{ in } \Omega(t) \text{ and } t \geq 0 \\ \nabla\Phi(t,\mathbf{x}) \cdot \mathbf{n} = 0 & \mathbf{x} \text{ on } \Gamma_w(t) \text{ and } t \geq 0 \\ \Phi(t,\mathbf{S}(t;\theta)) = \phi(t;\theta) & \theta \text{ in } [0,1] \text{ and } t \geq 0 \end{cases} \tag{1}$$

where $\nabla^2 = \partial^2/\partial x^2 + \partial^2/\partial y^2$, $\mathbf{n}$ is the outward normal on the boundary and $\phi(t;\theta)$ stands for the potential function along the free surface. The velocity vector $\mathbf{V} = (u,v)$ has horizontal $u = u(t,\mathbf{x})$ and vertical $v = v(t,\mathbf{x})$ components of velocity, apparently the derivatives of the potential: $\mathbf{V} = \nabla\Phi$. The parametric equations of the free surface evolution can be derived knowing the velocity field $\mathbf{V}_s$ on $\Gamma_s(t)$:

$$\frac{\partial \mathbf{S}}{\partial t}(t;\theta) = \mathbf{V}_s(t;\theta) \tag{2}$$

where $\mathbf{V}_s(t;\theta) = (u(t,\mathbf{S}(t;\theta)), v(t,\mathbf{S}(t;\theta)))^T$. Assuming constant atmospheric pressure acting on the free surface, the boundary condition on the free streamline is given by:

$$\frac{\partial \phi}{\partial t}(t;\theta) = \frac{1}{2}\left\|\mathbf{V}_s(t;\theta)\right\|^2 \tag{3}$$

where $\|\mathbf{V}_s\| = \sqrt{\mathbf{V}_s \cdot \mathbf{V}_s}$ is the familiar Euclidean norm. Equation (1) is used to compute $\mathbf{V}_s(t;\theta)$. At the initial time $t = 0$ the surge strikes the wall and the free surface is then deflected upward. The calculation was started with the liquid already in contact with the wall. The initial condition provides the

starting value of the potential: $\Phi(0,\mathbf{x}) = \Phi_0(\mathbf{x})$, $\mathbf{x}$ in $\Omega(0)$ and on the free surface: $\mathbf{S}(0;\theta) = \mathbf{S}_0(\theta)$, $\phi(0;\theta) = \Phi_0(\mathbf{S}_0(\theta))$, θ in $[0,1]$. The potential of the initial flow field will be specified in the section dealing with the numerical simulation.

4 The solution algorithm

The domain of definition of θ is divided into $N-1$ equal intervals: $0 = \theta_1 < \cdots < \theta_N = 1$. The computational domain $\Omega(t)$ is approximated by $\Omega_h(t)$, whose closed boundary $\partial\Omega_h(t)$ is piecewise linear; $\Omega_h(t)$ is then triangulated by the mesh generator TRIANGLE (see `http:// almond.srv.cs.cmu.edu /afs/cs/project/quake/public/www/triangle.html`). The set of the generated triangles is assumed regular (1). The nodes of the mesh belonging to the free surface are numbered from 1 to N, while the remaining ones are numbered from $N+1$ to K. The number N is set at the beginning of the computation, while $K(n)$ is a number that is controlled by the partition generated at the $n-$th time step. Some definitions are useful for the sake of conciseness: $\mathbf{S}_i(t) = \mathbf{S}(t;\theta_i)$, $\phi_i(t) = \phi(t;\theta_i)$, $\mathbf{V}_i(t) = \mathbf{V}_s(t;\theta_i)$. Evaluating (2) and (3) on θ_i, the following discrete formulation for the free surface location and potential is obtained:

$$\frac{\partial \mathbf{S}_i}{\partial t} = \mathbf{V}_i\,, \qquad \frac{\partial \phi_i}{\partial t} = \frac{1}{2}\left\|\mathbf{V}_i\right\|^2\,, \qquad i = 1,2,\ldots,N$$

It is assumed that the free surface location $\mathbf{S}_i^n$ and the potential along the free surface ϕ_i^n are known at the time t^n. The time marching is performed by the Crank and Nicolson method by evaluating the free surface and the surface potential at time t^{n+1} at any node $i\,(i = 1,2,\ldots,N)$:

$$\mathbf{S}_i^{n+1} = \mathbf{S}_i^n + \frac{\Delta t}{2}\left(\mathbf{V}_i^n + \mathbf{V}_i^{n+1}\right), \quad \phi_i^{n+1} = \phi_i^n + \frac{\Delta t}{4}\left(\left\|\mathbf{V}_i^n\right\|^2 + \left\|\mathbf{V}_i^{n+1}\right\|^2\right)$$

The implicit nature of the Crank and Nicolson scheme calls for an iterative procedure to be started with the initial values $\mathbf{S}_i^{n+(0)} = \mathbf{S}_i^n$ and $\phi_i^{n+(0)} = \phi_i^n$; the iteration then proceeds until convergence is reached using the following fixed point procedure:

$$\mathbf{S}_i^{n+(\ell+1)} = \alpha\mathbf{S}_i^n + (1-\alpha)\mathbf{S}_i^{n+(\ell)} + \alpha\frac{\Delta t}{2}\left(\mathbf{V}_i^n + \mathbf{V}_i^{n+(\ell)}\right), \tag{4a}$$

$$\phi_i^{n+(\ell+1)} = \alpha\phi_i^n + (1-\alpha)\phi_i^{n+(\ell)} + \alpha\frac{\Delta t}{4}\left(\left\|\mathbf{V}_i^n\right\|^2 + \left\|\mathbf{V}_i^{n+(\ell)}\right\|^2\right), \tag{4b}$$

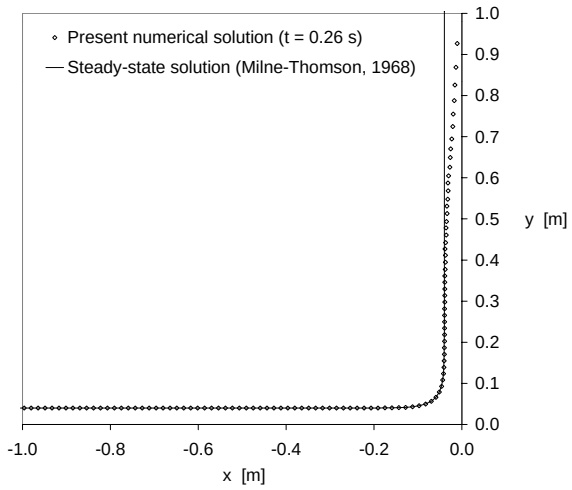

Figure 3: Evolution towards the steady state (flow is from left to right).

where $\ell = 0, 1, 2, \ldots, L$ is the sub-iteration index at each time step, and the relaxation parameter $\alpha = 0.5$ was used in the present calculation. At convergence $\mathbf{S}_i^{n+1} = \mathbf{S}_i^{n+(L+1)}$ and $\phi_i^{n+1} = \phi_i^{n+(L+1)}$, where L turned out to be typically less than 10. The treatment of the numerical instabilities of the free surface has been pursued in this work by modifying the free surface evolution equation (2) as follows:

$$\frac{\partial \mathbf{S}}{\partial t}(t;\theta) = \mathbf{V}_s(t;\theta) + \frac{1}{2N}\frac{\partial^2 \mathbf{S}}{\partial s^2}\left(\frac{\partial \mathbf{S}}{\partial \theta}\right)^{-1}$$

where $s(\theta) = \int_0^\theta \|d\mathbf{S}/d\theta\|\, d\theta$ is the arc length. The free surface nodal velocities $\mathbf{V}_i^n$ are estimated by solving numerically the problem (1); likewise for $\mathbf{V}_i^{n+(\ell)}$. A Finite Volume Element (FVE) scheme (4) has been implemented to solve problem (1), after the meshing of the domain $\Omega_h(t)$. The meshing of $\Omega_h(t^n)$ is performed by TRIANGLE, while the meshing of $\Omega_h(t^{n+(\ell)})$ is done by stretching the whole mesh computed at the time t^n.

The mesh manager useful to construct the FVE approximation has been performed by means of P2MESH (8), a free software package conceived for the fast development of Finite Volume and Finite Element codes on 2–D *unstructured* mesh. By modifying equation (4b) as follows:

$$\phi_i^{n+(\ell+1)} = \alpha\phi_i^n + (1-\alpha)\phi_i^{n+(\ell)} + \alpha\frac{\Delta t}{4}\|\mathbf{V}_i^n\|^2 + \alpha\frac{\Delta t}{4}\nabla\Phi_i^{n+(\ell)} \cdot \nabla\Phi_i^{n+(\ell+1)}$$

the coupling of the discretized version of eqns. (1) and (4b) is improved. This

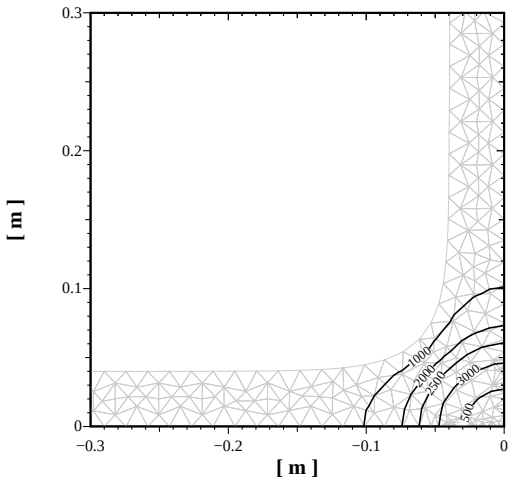

Figure 4: Isobars at 0.26 s (flow is from left to right; pressure in Pascal).

modification only slightly increases the computational cost because its effect is to add just few coefficients in some rows of the resulting linear system.

5 Results of the numerical simulations

5.1 Validation of the numerical model

The code has been at first validated by means of the steady state solution (6); fig. 3 shows how the unsteady free surface profile is clearly evolving towards the steady jet. The isobars are illustrated in fig. 4, where the symmetry about the bisectrix of the axes has been reached by the numerical liquid jet. This symmetry feature is embodied by the steady state analytical solution. The computed wall pressure evolves towards a steady state (Fig. 5).

5.2 Application of the numerical model

The complete simulation of the dam-break surge, starting from the removal of the gate and proceeding towards the impact wall, would clearly provide the suitable flow field to start the calculation of the impact; but this is beyond the scope of the present work, which is simply to demonstrate the feasibility of a potential flow model to reproduce the bore impact. The laboratory experimental impact chosen to run the numerical model has been derived from one of the clear water impacts detailed in (14) and in (15). The initial condition for the flow field is not known from the physical experiments; instead, only

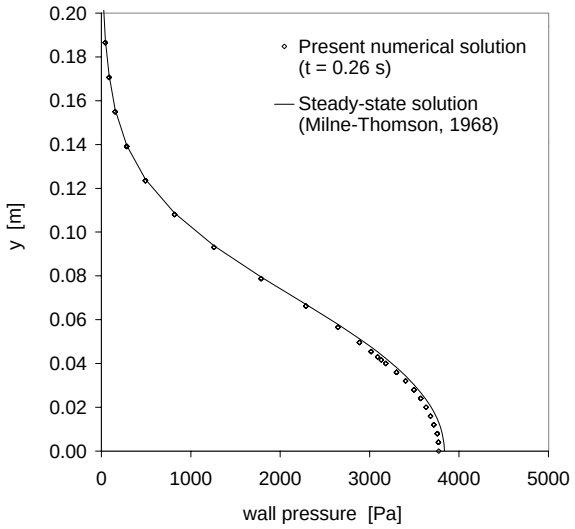

Figure 5: Wall pressure evolves towards the steady state.

the *toe* velocity $u_o = 2.77\,m/s$ was measured, apparently a rough estimate of the whole flow. This quantity is the picture of an instant of time and it can hardly represent a highly unsteady phenomenon. It is to be recalled that the measurements of *instantaneous* toe velocities were performed by tracing the location of the most advanced part of the ever–breaking front rushing downstream; therefore toe velocities do embody huge turbulent streamwise fluctuations, which are estimated to be as high as $\pm 10\%$ the average velocity. The 1–D Ritter's solution (13) was then adopted as the initial condition for the flow field; the front region is simulated by a trapezoidal domain moving at constant velocity $u_o = 2.77\,m/s$ (Fig. 6). This initial computational domain is a good approximation of the mildly elongated physical toe, as it was observed in the video pictures of the experiments. Air entrainment and gravity have both been neglected in the numerical computations. By trial

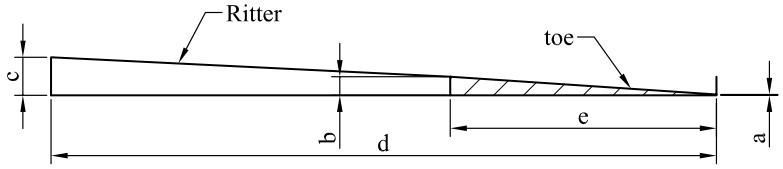

Figure 6: Initial domain (a=1 mm; b= 2.8 mm; c=6.3 mm; d=1m; e= 0.4cm)

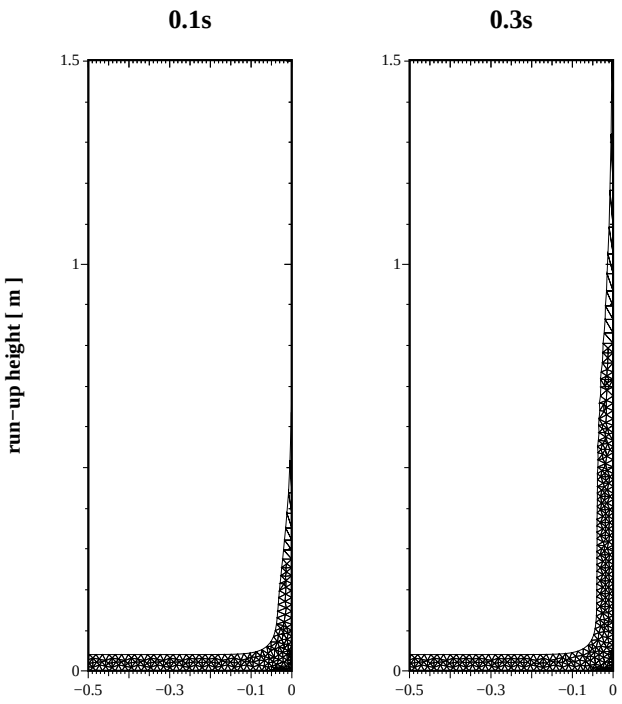

Figure 7: grids at 0.1 and 0.3 s (flow is from left to right).

and error a convenient temporal step was found to be $10^{-4}\,s$. The typical number of generated triangles was 1000; the typical CPU time for a complete simulation, involving $3.5 \cdot 10^3$ time steps, was half an hour in an ordinary 500 Mhz processor. The grid is depicted in Fig. 7; the model predicts the moving free surface while verifying closely the mass conservation, the maximum error being well less than 1%. It has to be pointed out that the accurate modeling of the free surface is not important as far as the calculation of the wall pressure is concerned; in fact it was observed in the present numerical simulation that different schematizations of the impacting liquid shape affect the wall pressure evolution by a small amount, which is a result of relevant value in practical circumstances. The free surface comparison (Fig. 8) shows a clear discrepancy between the numerical and the physical profile due to the huge air entrainment, phenomenon which has not been accounted for in the numerical simulation; nevertheless it will be shown that the wall force is predicted well (Fig. 9). The tiny oscillations of the force evolution are due to the nodes of the moving mesh (which is rebuilt at any time step) passing through the numerical gauge's location. The pressure on the wall is illustrated in Fig. 10. The knowledge of the wall force is normally the most relevant quantity for design; the force acting on the rigid surface was

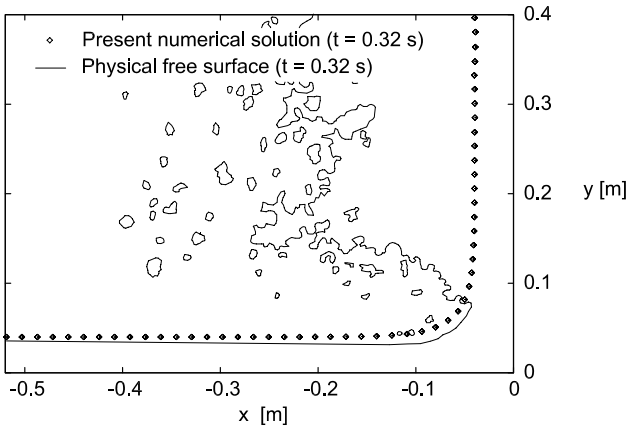

Figure 8: Measured and computed free surface (flow is from left to right).

obtained by integrating the pressure diagrams, (15).

6 Conclusions

The aim of the present study is to explore the possibility to evaluate the wall force with reasonable accuracy from rather simplified assumptions of the collision process. The very first version of the code was a simple one, since it was based on a semi–implicit method with *no* numerical technique to smooth the free surface. Roughly at the time $0.2\,s$ a sort of sawtooth instability started to develop on the free streamline, but remained limited in size and did not increase; at the end of the $1\,s$ simulation the code was still stable. In spite of the free surface instabilities, the pressure and the wall force were predicted with as much accuracy as the results presented in section 5, that were obtained by the final version of the code, which included the full implicit scheme, the smoothing treatment of the free surface and a more realistic initial condition. The range of validity of the model, as far as the wall force is concerned, is much larger than it could be initially suspected: even an initial condition as unrealistic as the "face-to-face" impact (a rectangular domain with constant velocity everywhere) was capable of giving the wall force evolution of fig. 9, apart from the very early stage of the impact. The air entrainment in the bore, before and after the impact, has been neglected in the numerical simulation and yet the wall force is reproduced accurately; so it is suggested that as long as the air concentration in the toe is low, as it was in the present experimental runs, air entrainment has no effect on the wall quantities.

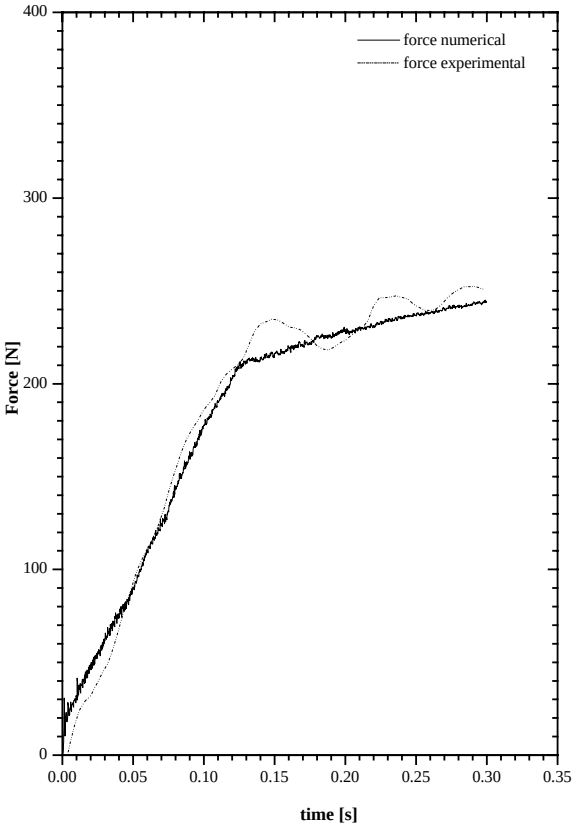

Figure 9: Temporal evolution of the wall force.

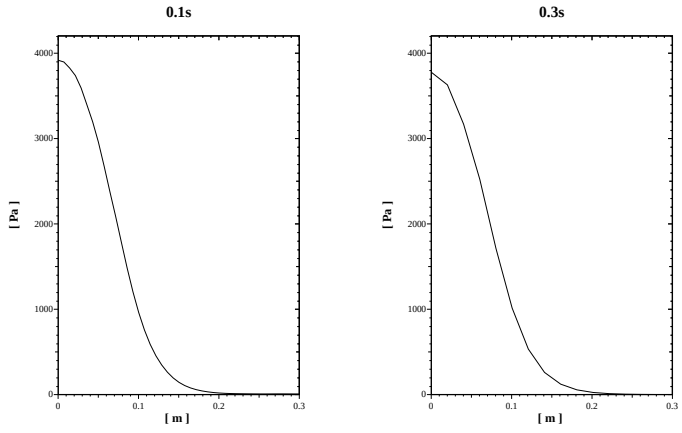

Figure 10: Wall pressure at 0.1 and 0.3 s.

While the present numerical model needs to be thoroughly corroborated by more realistic 2–D initial conditions, it seems capable of reproducing with accuracy the non–linear impact of a dam–break surge and so there are reasons to believe that, at least as far as the wall force and bending moment are concerned, meaningful predictions for the prototype can be obtained not only from laboratory tests but also from numerical simulations, considering also the order of magnitude of the errors involved even in the experimental laboratory measurements.

The animation of the impact, based on the present numerical simulation, can be watched and downloaded at the following URL :
`http://www.ing.unitn.it/~bertolaz/numerical/index.html`

References

[1] P.G. Ciarlet,
"The finite element method for elliptic problems",
North-Holland Publishing Company, Amsterdam, Holland, 1980.

[2] R.H. Cross,
"Tsunamis surge forces",
J. of the Waterways and Harbor Div., ASCE, 93 (WW4), 201–231, 1967.

[3] J.W. Dold, D.H. Peregrine,
"An efficient boundary–integral method for steep unsteady water waves",
Proceedings, in Numerical Methods for Fluid Dynamics, Editions Morton K.W.&Baines, Oxford University Press, Great Britain, 671–679, 1986.

[4] J. Huang, S. Xi,
"On the finite volume element method for general self-adjoint elliptic problems",
SIAM Journal on Numerical Analysis, vol. 35, 5, 1762–1774, 1998.

[5] M.S. Kirkgöz,
"Shock pressure of breaking waves on vertical walls",
J. of Waterways, Port, Ocean Eng. Division, ASCE, 108, 81–95, 1982.

[6] L.M. Milne–Thompson,
"Theoretical Hydrodynamics,",
5th Edition, MacMillan, New York, 1968.

[7] P.K. Mohapatra, S.M. Bhallamudi, V. Eswaran,
"Numerical simulation of impact of bores against inclined walls",
Journal of Hydraulic Engineering, vol. 126, 12, 942–945, 2000.

[8] E. Bertolazzi, G. Manzini,
"Algorithm xxx: P2MESH: Generic Object-oriented Interface Between 2-D Unstructured Meshes and FEM/FVM-based PDE Solvers",
ACM Transactions on Mathematical Software (accepted).

[9] D.H. Peregrine, M.E. Topliss,
"The impact of water waves upon a wall",
Proceedings of the IUTAM/ISIMM Symposium on Structure and Dynamics of Nonlinear Waves in Fluids, 17–20 August, 83–98, 1994.

[10] D.H. Peregrine, L. Thais,
"The effect of entrained air in violent water wave impacts",
Journal of Fluid Mechanics, vol. 325, 377–397, 1996.

[11] J.D. Ramsden, F. Raichlen,
"Forces on vertical wall caused by incident bores",
J. of Waterway, Port, Coastal and Ocean Eng., vol. 116, 5, 592–613, 1990.

[12] N.S.G. Rao, H. Kobus,
"Characteristics of self–aerated free–surface flows ",
Water and Waste Water, Current Research and Practice,vol.10, Erich Schmidt Verlag, Berlin, Germany, 1973.

[13] A. Ritter,
"Die Fortpflanzung der wasserwellen",
Zeitschrift des vereines deutscher ingenieure, vol. 36, 33, 947–954, 1892 (in german).

[14] P. Scotton,
"Dynamic impact of debris flow: experimental study",
IDR2, Dept. of Civil and Environmental Eng., Trento, Italy, 1996.

[15] F. Trivellato, P. Scotton,
"Bore impact upon a wall (experimental database)",
Dept. of Civil and Environmental Engineering, Trento, Italy, 2001.

[16] S. Zhang, D.K.P. Yue, K. Tanizawa,
"Simulation of plunging wave impact on a vertical wall ",
Journal of Fluid Mechanics, 327, 221–254, 1996.